Direct Power Control of PWM Converter without Power Source Voltage Sensors

Toshihiko Noguchi, *Member, IEEE*, Hiroaki Tomiki,
Seiji Kondo, *Member, IEEE*, and Isao Takahashi, *Fellow, IEEE*

Nagaoka University of Technology
1603-1 Kamitomioka, Nagaoka 940-21, Japan
Phone : 81-258-46-6000, Fax : 81-258-46-6506, E-mail : omom@voscc.nagaokaut.ac.jp

***Abstract*—This paper proposes a novel control strategy of a PWM converter with no power source voltage sensors. The strategy has two features to improve a total power factor including harmonic components without detecting the voltages. One is an estimation technique of the power source voltages, which can estimate instantaneous values of the voltages by evaluating instantaneous active and reactive power according to every switching mode of the converter. The other is a direct instantaneous power control technique, which can directly control the instantaneous active and reactive power by using switching modes as manipulated values for the converter.**

A DSP based experimental system was developed, and experimental tests were conducted. The control period of the system was only $15\mu s$. It was confirmed that the maximum total power factor was more than 99%, and the maximum efficiency was 96.2%. The results have proven excellent performance of the proposed system.

I. INTRODUCTION

OWING to prevalence of power electronic systems, many problems with regard to diode rectifiers have arisen in recent years. One of the problems is a low input power factor, and another is current harmonics. These are reasons why PWM converters are adopted in such particular applications that strict regulations are imposed to reduce the waveform distortion. The PWM converters can not only reduce the harmonic components of the input currents but also easily control the currents to make the unity power factor possible [1].

A conventional control technique of the PWM converter was based on ac current control of which commands were provided by the detected power source voltages [2]. In general, the converter requires three kinds of sensors to control the ac currents and the dc-bus voltage as follows:

1) ac current sensors for current control (Hall effect sensors);

2) dc-bus voltage sensor for regulating the dc-bus (an isolation amplifier or a photo coupler);

3) power source voltage sensors for the unity power factor control (transformers or photo couplers).

The sensors of 1) and 2) are essential for not only control but also system protection [3]. On the other hand, it is desirable to eliminate the voltage sensors of 3) to simplify the system configuration and to improve the system reliability.

This paper proposes a novel control technique of the PWM converter, which enables the converter to achieve the unity power factor without any power source voltage sensors. The technique consists of two concepts. One is an estimation technique of the power source voltages, and the other is a direct instantaneous power control technique of the converter. The voltage estimation is based on instantaneous active and reactive power of the power source according to a specific switching mode of the converter. Since the method deals with instantaneous variables, it is possible to estimate not only a fundamental component [4] but also harmonic components. The direct instantaneous power control of the converter is a quite different technique comparing with current control based conventional techniques [5]. The proposed technique enables the converter to control not the line currents but directly the instantaneous active and reactive power. The system is based on relay-type control of the power with hysteresis elements and optimization of converter switching modes by using a switching table.

In the paper, theoretical analysis is developed with regard to the above sensorless system, and several experimental results are presented to verify feasibility of the proposed technique.

II. PRINCIPLES OF DIRECT POWER CONTROL WITHOUT POWER SOURCE VOLTAGE SENSORS

A. Power Source Voltage Estimation Method

Figure 1 shows a power circuit of the PWM converter to be studied, where symbols are listed below:

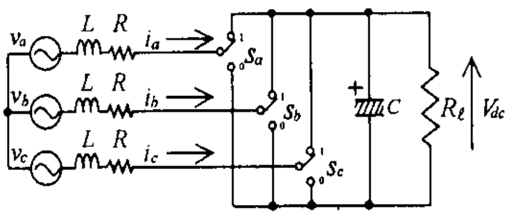

Fig. 1. Diagram of a three-phase PWM converter.

0-7803-3544-9/96 $5.00 © 1996 IEEE

TABLE I
RELATIONS BETWEEN SWITCHING MODE AND ESTIMATING EQUATIONS OF INSTANTANEOUS ACTIVE AND REACTIVE POWER

S_a, S_b, S_c	$\hat{p}$	$\hat{q}$
1, 0, 0	$L(\frac{\mathrm{d}i_a}{\mathrm{d}t}i_a+\frac{\mathrm{d}i_b}{\mathrm{d}t}i_b+\frac{\mathrm{d}i_c}{\mathrm{d}t}i_c)+V_{dc}i_a$	$\frac{1}{\sqrt{3}}[3L(\frac{\mathrm{d}i_c}{\mathrm{d}t}i_b-\frac{\mathrm{d}i_b}{\mathrm{d}t}i_c)-V_{dc}(i_b-i_c)]$
1, 1, 0	$L(\frac{\mathrm{d}i_a}{\mathrm{d}t}i_a+\frac{\mathrm{d}i_b}{\mathrm{d}t}i_b+\frac{\mathrm{d}i_c}{\mathrm{d}t}i_c)-V_{dc}i_c$	$\frac{1}{\sqrt{3}}[3L(\frac{\mathrm{d}i_b}{\mathrm{d}t}i_a-\frac{\mathrm{d}i_a}{\mathrm{d}t}i_b)+V_{dc}(i_a-i_b)]$
0, 1, 0	$L(\frac{\mathrm{d}i_a}{\mathrm{d}t}i_a+\frac{\mathrm{d}i_b}{\mathrm{d}t}i_b+\frac{\mathrm{d}i_c}{\mathrm{d}t}i_c)+V_{dc}i_b$	$\frac{1}{\sqrt{3}}[3L(\frac{\mathrm{d}i_a}{\mathrm{d}t}i_c-\frac{\mathrm{d}i_c}{\mathrm{d}t}i_a)-V_{dc}(i_c-i_a)]$
0, 1, 1	$L(\frac{\mathrm{d}i_a}{\mathrm{d}t}i_a+\frac{\mathrm{d}i_b}{\mathrm{d}t}i_b+\frac{\mathrm{d}i_c}{\mathrm{d}t}i_c)-V_{dc}i_a$	$\frac{1}{\sqrt{3}}[3L(\frac{\mathrm{d}i_c}{\mathrm{d}t}i_b-\frac{\mathrm{d}i_b}{\mathrm{d}t}i_c)+V_{dc}(i_b-i_c)]$
0, 0, 1	$L(\frac{\mathrm{d}i_a}{\mathrm{d}t}i_a+\frac{\mathrm{d}i_b}{\mathrm{d}t}i_b+\frac{\mathrm{d}i_c}{\mathrm{d}t}i_c)+V_{dc}i_c$	$\frac{1}{\sqrt{3}}[3L(\frac{\mathrm{d}i_b}{\mathrm{d}t}i_a-\frac{\mathrm{d}i_a}{\mathrm{d}t}i_b)-V_{dc}(i_a-i_b)]$
1, 0, 1	$L(\frac{\mathrm{d}i_a}{\mathrm{d}t}i_a+\frac{\mathrm{d}i_b}{\mathrm{d}t}i_b+\frac{\mathrm{d}i_c}{\mathrm{d}t}i_c)-V_{dc}i_b$	$\frac{1}{\sqrt{3}}[3L(\frac{\mathrm{d}i_a}{\mathrm{d}t}i_c-\frac{\mathrm{d}i_c}{\mathrm{d}t}i_a)+V_{dc}(i_c-i_a)]$
0, 0, 0	$L(\frac{\mathrm{d}i_a}{\mathrm{d}t}i_a+\frac{\mathrm{d}i_b}{\mathrm{d}t}i_b+\frac{\mathrm{d}i_c}{\mathrm{d}t}i_c)$	$\frac{1}{\sqrt{3}}[3L(\frac{\mathrm{d}i_b}{\mathrm{d}t}i_a-\frac{\mathrm{d}i_a}{\mathrm{d}t}i_b)]$
1, 1, 1	$L(\frac{\mathrm{d}i_a}{\mathrm{d}t}i_a+\frac{\mathrm{d}i_b}{\mathrm{d}t}i_b+\frac{\mathrm{d}i_c}{\mathrm{d}t}i_c)$	$\frac{1}{\sqrt{3}}[3L(\frac{\mathrm{d}i_b}{\mathrm{d}t}i_a-\frac{\mathrm{d}i_a}{\mathrm{d}t}i_b)]$

v_a, v_b and v_c three-phase voltages of the ac power source;
i_a, i_b and i_c three-phase line currents;
S_a, S_b and S_c switching states of the converter;
V_{dc} dc-bus voltage;
L inductance of an interconnecting reactor;
R resistance of the interconnecting reactor;
C smoothing capacitor across the dc-bus;
R_ℓ load resistor.

In order to make the following discussion easier, it is assumed that switching devices are functionally ideal and do not require dead time to prevent a short circuit at the dc-bus.

An instantaneous voltage vector v and an instantaneous current vector i are defined as

$$v = v_\alpha + \mathrm{j}v_\beta = \sqrt{\frac{2}{3}}\left(v_a + v_b e^{\mathrm{j}2\pi/3} + v_c e^{\mathrm{j}4\pi/3}\right) \quad (1)$$

$$i = i_\alpha + \mathrm{j}i_\beta = \sqrt{\frac{2}{3}}\left(i_a + i_b e^{\mathrm{j}2\pi/3} + i_c e^{\mathrm{j}4\pi/3}\right), \quad (2)$$

where
v_α and v_β two-phase components of the voltage vector;
i_α and i_β two-phase components of the current vector.

Using the instantaneous vectors defined above, instantaneous apparent power s can be defined as follows:

$$s = v\bar{i} = p + \mathrm{j}q$$
$$= v_a i_a + v_b i_b + v_c i_c + \mathrm{j}\frac{1}{\sqrt{3}}\left[(v_b - v_c)i_a + (v_c - v_a)i_b + (v_a - v_b)i_c\right], \quad (3)$$

where variables and symbols are described as
p instantaneous active power;
q instantaneous reactive power;
$\bar{x}$ conjugate of a vector x.

It is known that the calculation of p is a scalar product between the three-phase voltages and currents, whereas q is a vector product between them.

It is possible to calculate the phase voltages by simply adding converter output voltage vectors to voltage drops in the interconnecting reactors. Since the neutral point potential of the power supply is not given, however, variations of the neutral point in the converter has to be considered to calculate the power source voltages. In order to avoid an intricate procedure for estimating the neutral point potential, the proposed method utilizes p and q as intermediate variables to estimate the power source voltages. In addition, the estimated p and q can be effectively used in the PWM converter for directly controlling the active and reactive power as described in the next section. However, (3) requires the power source voltages to evaluate p and q, which are ought to be eliminated to achieve sensorless operation. Rewriting p and q with the three-phase line currents, dc-bus voltage, and the inductance values of the interconnecting reactors instead of the power source voltages, $\hat{p}$ and $\hat{q}$ can be estimated as shown in TABLE I. In the following discussion, when a calculation requires parameters of the interconnecting reactors, a notation for estimated values is used as :
$\hat{x}$ estimated value of x.

As can be seen in TABLE I, it is found that the estimating equation for $\hat{p}$ and $\hat{q}$ has to be changed according to a specific switching mode of the converter, and each equation requires the inductance value L as a system parameter. In the strict sense, the resistance value R of the interconnecting reactors should also be considered to estimate the power. However, power regarding R is relatively small comparing it with the active power of the dc-bus and the reactors, and R has no relation with the estimation of $\hat{q}$. This is the reason why R is neglected in TABLE I. After estimating $\hat{s}$ ($= \hat{p} + \mathrm{j}\hat{q}$) on the basis of TABLE I, the voltage vector $\hat{v}$ can be estimated as

$$\hat{v} = \frac{i}{|i|^2}\hat{s}, \quad (4)$$

where
$|x|$ amplitude (norm) of a vector x.

In general, the amplitude of i is not zero, because the dc-bus is loaded by R_ℓ; hence (4) can be solved with respect to $\hat{v}$. Equation (4) can be rewritten in a concrete form using two-phase components as

$$\begin{bmatrix} \hat{v}_\alpha \\ \hat{v}_\beta \end{bmatrix} = \frac{1}{{i_\alpha}^2 + {i_\beta}^2} \begin{bmatrix} i_\alpha & -i_\beta \\ i_\beta & i_\alpha \end{bmatrix} \begin{bmatrix} \hat{p} \\ \hat{q} \end{bmatrix}. \tag{5}$$

The three-phase power source voltages can be easily obtained from (5) by using two-phase to three-phase conversion. Since the proposed estimation method is based entirely on the instantaneous variables, it can estimate not only a fundamental component but also harmonic components of the power source voltages. Therefore, the method has an advantage over the conventional technique in terms of total power factor improvement.

B. Sensorless Direct Power Control of PWM Converter

Figure 2 shows an example of the voltage sensorless PWM converter using the proposed voltage estimation method. The control strategy shown in Fig. 2 is direct instantaneous power control of the converter. The strategy is based on relay-type control of the instantaneous active and reactive power, and the power is directly controlled by switching modes of the converter. Therefore, it is possible for the converter to achieve the unity power factor by controlling the reactive power to be zero. The estimated $\hat{p}$ and $\hat{q}$ are utilized as feedback signals. The active power command p^* is provided by a dc-bus voltage control block, while the reactive power command q^* is directly provided as an external signal. Differences between the command values and the estimated values are quantized by using hysteresis elements. The quantized signals are represented as S_p and S_q respectively. Also, the region of the estimated voltage vector is divided into twelve sectors as shown in Fig. 3.

$$(n-2)\frac{\pi}{6} \le \Theta_n < (n-1)\frac{\pi}{6} \qquad \because n = 1,2,\cdots,12 \tag{6}$$

The quantized signals S_p, S_q and Θ_n are input to a switching table shown in TABLE II, and an optimum switching mode S_a, S_b and S_c can be selected uniquely according to a combination of the input signals.

The voltage estimation method proposed in the previous section can also be applicable to the conventional current regulated PWM converter as shown in Fig. 4. The converter adopts a current controller with subharmonic modulation. The unity power factor is achieved by conforming the current phase to the estimated voltage phase. In case of the configuration, the estimated voltages are utilized to provide current commands. Performance comparison between the two systems of Fig. 2 and Fig. 4 is presented in the next chapter.

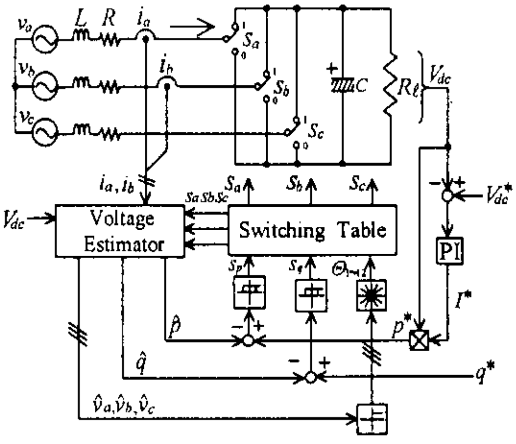

Fig. 2. Block diagram of the direct instantaneous power control of the PWM converter without power source voltage sensors.

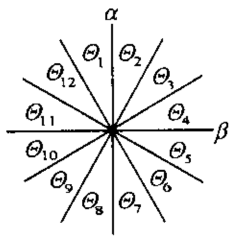

Fig. 3. $\alpha-\beta$ plane divided into twelve sectors to detect the phase of the voltage vector.

TABLE II
SWITCHING TABLE FOR DIRECT INSTANTANEOUS POWER CONTROL

S_p	S_q	Θ_1	Θ_2	Θ_3	Θ_4	Θ_5	Θ_6	Θ_7	Θ_8	Θ_9	Θ_{10}	Θ_{11}	Θ_{12}
1	0	101	101	100	100	110	110	010	010	011	011	001	001
	1	110	111	010	000	011	111	001	000	101	111	100	000
0	0	101	100	100	110	110	010	010	011	011	001	001	101
	1	100	110	110	010	010	011	011	001	001	101	101	100

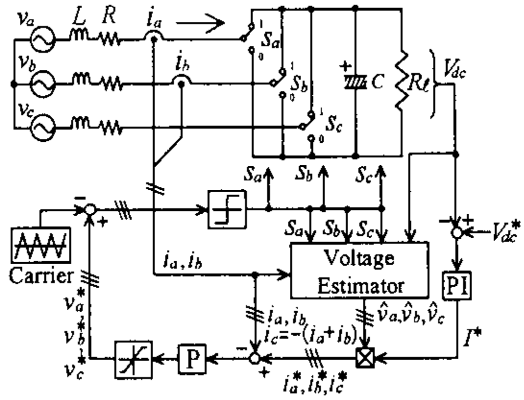

Fig. 4. Block diagram of the conventional control of the PWM converter without power source voltage sensors.

TABLE III
ELECTRICAL PARAMETERS OF THE POWER CIRCUIT

Resistance of the reactor R	0.2 [Ω]
Inductance of the reactor L	11.5 [mH]
Smoothing capacitor C	4700 [μF]
Load resistor R_ℓ	100 [Ω]
Switching frequency f_{sw}	8 [kHz]
Power devices	IGBT
Power source voltage and frequency	200 [V], 50 [Hz]
Dc-bus voltage command V_{dc}^*	283 [V]

III. EXPERIMENTAL SYSTEM AND RESULTS

A. System configuration

Two experimental systems were developed to compare their performances. One is based on the direct instantaneous power control, and the other is based on the conventional current control with subharmonic modulation. Both systems, however, utilizes a same power circuit.

The power circuit of the converter is constituted by an IGBT

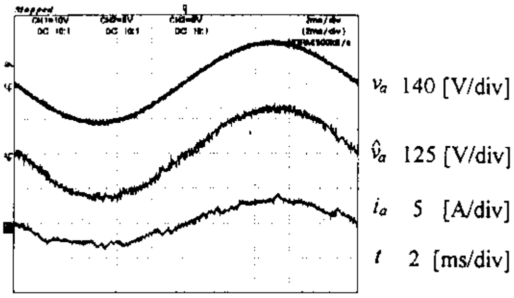

(a) Power source voltage, the estimated voltage and the line current.

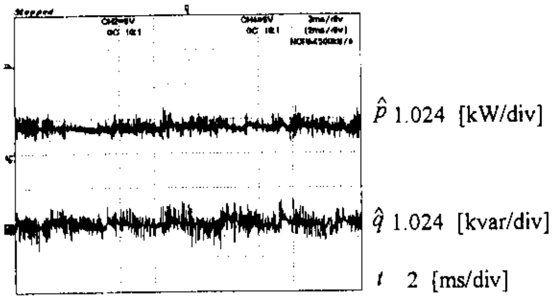

(b) Instantaneous active and reactive power.

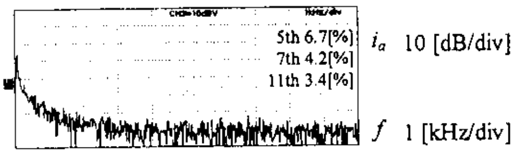

(c) Frequency spectra of the line current.

Fig. 5. Waveforms of the direct instantaneous power control in the steady state under the condition of the unity power factor.

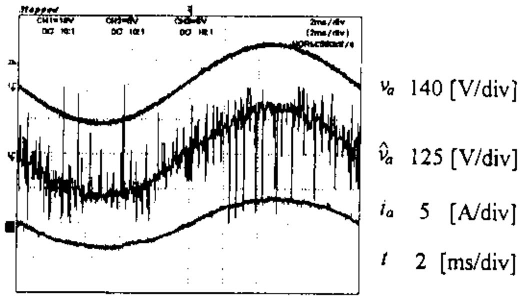

(a) Power source voltage, the estimated voltage and the line current.

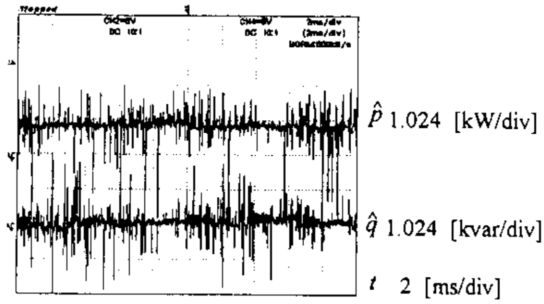

(b) Instantaneous active and reactive power.

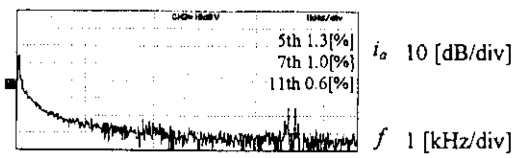

(c) Frequency spectra of the line current.

Fig. 6. Waveforms of the conventional control in the steady state under the condition of the unity power factor.

based full-bridge circuit of which electrical devices are shown in TABLE III. Two Hall effect sensors are used to detect the line currents, and an isolation amplifier is adopted to detect the dc-bus voltage. Most of the control circuits except PWM circuits are constituted by digital hardware. The estimation of the instantaneous power and the voltages is proceeded by DSP (TMS320C50-40MHz) software. The estimation program is executed in every $15\mu s$ control period initiated by an internal timer of the DSP. It is necessary to make the control intervals as short as possible, because the estimation algorithm has to be changed according to the switching modes of the converter as shown in TABLE I. Interface circuits which deal with detection of the line currents are designed to realize fast operation corresponding to the DSP processing; hence high sampling-rate and high-resolution A/D converters (ADS-231-12bit-1.5MS/s) are used in the system.

B. Experimental results

Several experimental tests were carried out to confirm feasibility of the proposed technique. Figure 5 shows experimental results of the direct instantaneous power control in the steady state under the condition of the unity power factor. Power dissipated in the load resistor was 810W. From Fig. 5(a), it is found that the power source voltage is successfully estimated, and the line current is in phase with the actual power source voltage. However, the current waveform slightly contains low order harmonic components. Since the feedback signals of the estimated power and voltages are provided discretely by the DSP, discrete time system based error causes the distortion in the current waveform. As shown in Fig. 5(b), the estimated active power indicates almost the same value as the load power, and the estimated reactive power is found to be zero. Figure 5(c) shows frequency spectra of the line current obtained with an FFT analyzer. The fifth, seventh and eleventh harmonic components are also identified in the figure. The current waveform distortion results in increase of the lower harmonics, but any conspicuous components are not observed at higher frequency region like a white noise.

On the other hand, Fig. 6 shows the results of the conventional current control system, and the operating condition was same as that of the direct instantaneous power control. As can be seen in Fig. 6(a), many ripples are observed in the estimated voltage signal, because the estimation in the DSP is asynchronous with the carrier in the PWM block. However, the line current is successfully controlled owing to the low gain of the current control loop at the frequency of the ripples. The estimated active and reactive power also includes many ripples as shown in Fig. 6(b). The average value of the estimated active power almost conforms to the actual power which is dissipated in the load resistor. Figure 6(c) shows the frequency spectra of the line current. It is found that the lower harmonic components of the method are approximately $2.8 \sim 5.4\%$ less than those of the direct instantaneous power control. However, side band components of the 8kHz carrier are remarkable.

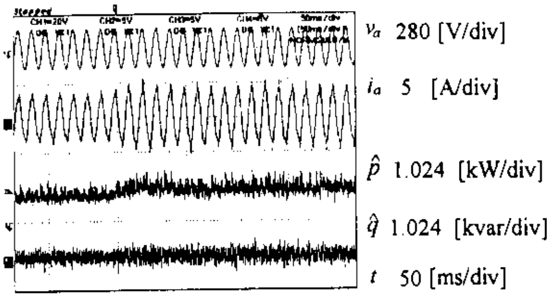

(a) Direct instantaneous power control.

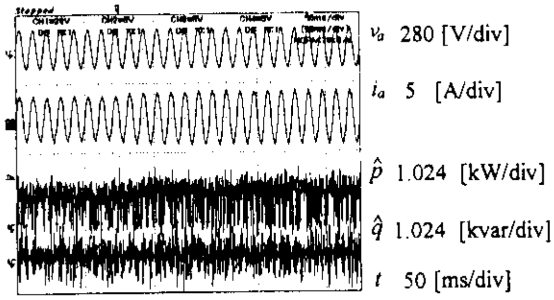

(b) Conventional control with subharmonic modulation.

Fig. 7. Step responses of the two methods under the condition of the unity power factor.

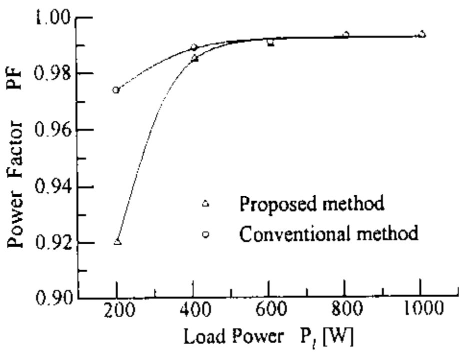

(a) Total power factor.

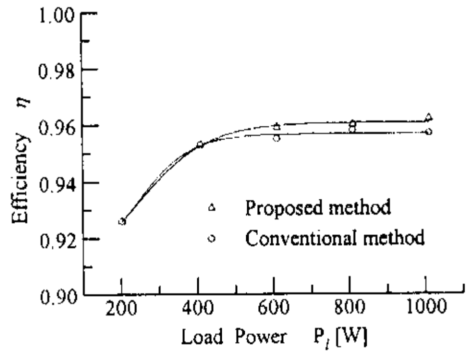

(b) Efficiency.

Fig. 8. Total power factor and efficiency of the two methods.

Figures 7(a) and 7(b) show the results of the both methods in the transient state under the condition of the unity power factor. The load power was changed stepwise from 750W to 900W in the experiment. It can be observed that the unity power factor control is achieved stably even in the transient, and it is found that the proposed methods are effective not only in the steady state but also in the transient state owing to the instantaneous estimation of the power source voltages.

Figure 8(a) shows some plots of the total power factor against the load power. The maximum power factor of the both methods was more than 99% at heavy load region. However, the power factor decreases gradually according to the decrease of the load power, and the power factor of the direct instantaneous power control is approximately 5% less than that of the current control with subharmonic modulation at the load power of 200W. It is considered that the lower harmonics owing to the discrete time system based error detrimentally affect on the total power factor at light load. Figure 8(b) shows efficiency characteristics against the load power. The direct instantaneous power control demonstrates the maximum efficiency of 96.2%, while that of the current control is 95.7%. The efficiency of the two methods was more than 92% even in the light load of 200W.

Figures 9(a) and (b) show the waveforms where 5th harmonic component of 10% was intentionally superposed on the power source voltage. It is recognized that the power source voltage can be estimated including the superposed harmonic component, because the proposed estimation method deals with the instantaneous

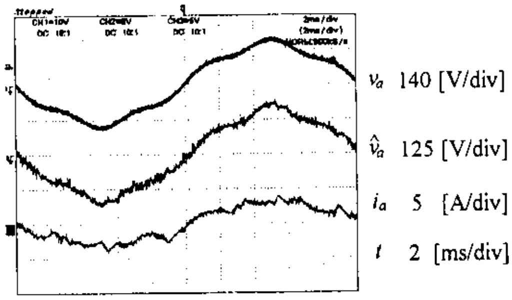

(a) Direct instantaneous power control.

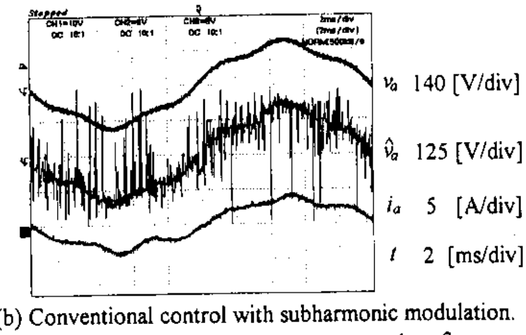

(b) Conventional control with subharmonic modulation.

Fig. 9. Estimation characteristics and control performance with 5th harmonic superposed on the power source voltage.

variables. In order to improve not only displacement factor but also total power factor, the waveform of the line current should be similar to that of the power source voltage as shown in Fig. 9(b). Although the power source voltage was successfully estimated, however, the line current of Fig. 9(a) did not follow very well the power source voltage. The reason of the deterioration is also owing to the discrete time system based error as described before.

Figures 10 and 11 show the waveforms of the direct instantaneous power control when the reactive power command was changed to ±500var. It was verified that the control could indirectly adjust the current phase through the reactive power command.

IV. CONCLUSION

The paper has described two kinds of concepts to improve total power factor of the PWM converter without power source voltage sensors. One is an estimation method of the power source voltages, and the other is a direct instantaneous power control of the converter. The voltage estimation method is based on evaluation of the instantaneous active and reactive power according to a specific switching mode of the converter. It is possible for the method to estimate the instantaneous values of the power source voltages. The direct instantaneous power control is based on relay-type control of the active and reactive power with hysteresis elements, and a switching table which consists of optimum switching modes of the converter is utilized to make the feedback power track their commands. The control can make it possible to disperse the frequency spectra of the line current harmonics and indirectly control the current phase by providing the reactive power command. Hence, combining the voltage estimation with the direct power control, total power factor including the harmonics can be improved without any voltage sensors. The experimental results of a prototype system have proven that the maximum total power factor was more than 99%, and the maximum efficiency was 96.2%.

REFERENCES

[1] T. Kataoka, K. Mizumachi, and S. Miyairi, "A Pulsewidth Controlled ac-to-dc Converter to improve Power Factor and Waveform of ac Line Current," *IEEE Trans. on Ind. App.*, vol. 15, no. 6, pp. 670-675, 1979.

[2] R. Wu, S. B. Dewan, and G. R. Slemon, "Analysis of a PWM ac to dc Voltage Source Converter under the Predicted Current Control with a Fixed Switching Frequency," *IEEE Trans. on Ind. App.*, vol. 27, no. 4, pp. 756-764, 1991.

[3] J. W. Dixon, and B-T. Ooi, "Indirect Current Control of a Unity Power Factor Sinusoidal Current Boost Type Three-Phase Rectifier," *IEEE Trans. on Ind. Elec.*, vol. 35, no. 4, pp. 508-515, 1988.

[4] T. Takeshita, T. Kobayashi, and N. Matsui, "A Scheme of Power Source Voltage Sensorless Three-Phase PWM AC/DC Converter," *IEEJ Trans. on Ind. App.*, vol. 114, no. 12, pp. 1211-1219, 1994.

[5] T. Noguchi, H. Tomiki, S. Kondo, and I. Takahashi, "Instantaneous Active and Reactive Power Control of PWM Converter by Using Switching Table," *IEEJ Trans. on Ind. App.*, vol. 116, no. 2, pp. 222-223, 1996.

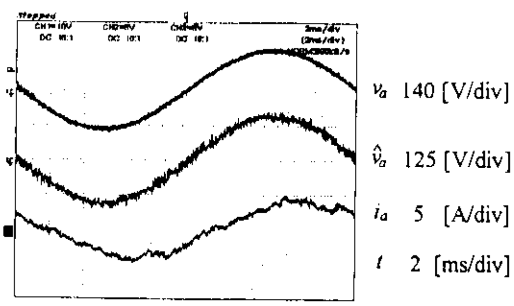

(a) Power source voltage, the estimated voltage and the line current.

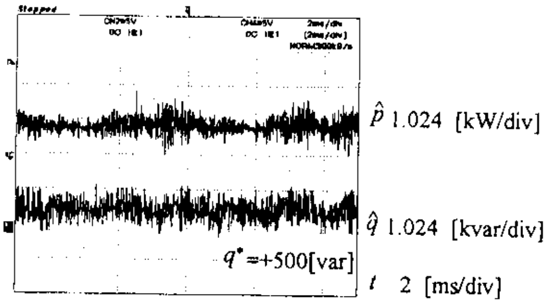

(b) Instantaneous active and reactive power.

Fig. 10. Lag power factor control by the proposed method.

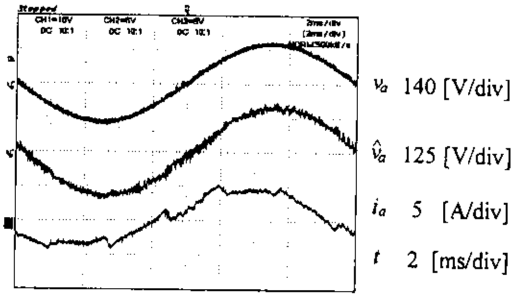

(a) Power source voltage, the estimated voltage and the line current.

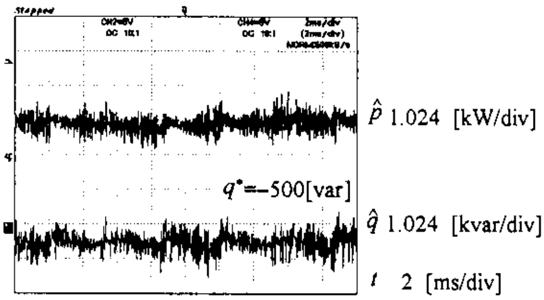

(b) Instantaneous active and reactive power.

Fig. 11. Lead power factor control by the proposed method.

APPENDIX

It is necessary for the proposed estimation to calculate differential values of the line currents on the basis of calculus of finite differences. Therefore, the calculation should not be executed during the period in which the switching mode of the converter changes. To avoid the problem, the switching signals in the direct instantaneous power control system are provided synchronously with the estimating operation in the DSP. This is the reason why the ripples of Fig. 6 are not observed in the estimated voltage waveform shown in Fig. 5.